Available online at www.sciencedirect.com
ScienceDirect
Electrochemistry Communications 9 (2007) 1127–1133
electrochemistry communications
www.elsevier.com/locate/elecom

Electro-deposition and stripping of catalytically active iron metal nanoparticles at boron-doped diamond electrodes

Veronica Saez [a], Jose Gonzalez-Garcia [a], M. Anbu Kulandainathan [b], Frank Marken [c,*]

[a] Universidad de Alicante, Departamento de Quimica Fisica, Grupo de Electroquim Aplicada, Ap. Correos 99, Alicante E-03080, Spain
[b] Central Electrochemical Research Institute, Karaikudi, Tamil Nadu 630 006, India
[c] Department of Chemistry, University of Bath, Bath BA2 7AY, UK

Received 9 December 2006; received in revised form 10 January 2007; accepted 11 January 2007
Available online 16 January 2007

Abstract

A new methodology for the electro-deposition and stripping of highly reactive iron nanoparticles at boron-doped diamond electrodes is proposed. In aqueous 1 M NH_4F iron metal readily and reversibly electro-deposits onto boron-doped diamond electrodes. The effects of deposition potential, FeF_6^{3-} concentration, deposition time, and mass transport are investigated. Power ultrasound (24 kHz, 8 W cm^{-2}) is employed to achieve enhanced mass transport conditions. Scanning electron microscopy images of iron nanoparticles grown to typically 20–30 nm diameter are obtained. It is shown that a strongly and permanently adhering film of iron at boron-doped diamond can be formed and transferred into other solution environments.

The catalytic reactivity of iron nanoparticle deposits at boron-doped diamond is investigated for the reductive dehalogenation of trichloroacetate. The kinetically limited multi-electron reduction of trichloroacetate is dependent on the FeF_6^{3-} deposition conditions and the solution composition. It is demonstrated that a stepwise iron catalysed dechlorination via dichloroacetate and monochloroacetate to acetate is feasible. This methodology in conjunction with power ultrasound offers a novel, clean, and very versatile electro-dehalogenation methodology. The role of fluoride in the surface electrochemistry of iron deserves further attention.

Keywords: Iron; Nanoparticle; Boron-doped diamond; Dehalogenation; Remediation; Ultrasound; Sonoelectrochemistry; Catalysis

1. Introduction

Boron-doped diamond has found a wide range of applications in electrochemistry due to its outstanding material properties [1,2]. In particular free-standing films of boron-doped diamond with high doping level have been employed in electroanalysis [3] and as an inert substrate for catalytically active metals [4] or metal oxides [5]. The intentional modification of the essentially inert boron-doped diamond surface has been employed in order to introduce specific catalytic activity for example with films or clusters of platinum [6], gold [7–10], TiO_2 [11], RuO_2 [12,13], cobalt oxide [14], and hydrous iridium oxide [15]. In this study the reversible deposition of stable deposits of iron and iron oxides at boron-doped diamond electrodes is demonstrated to give a sensitive analytic tool and a novel electro-catalytic dehalogenation function to the otherwise inert diamond electrode surface.

Iron nanoparticles are known to be highly reactive and they have been employed in processes such as dehalogenation and remediation [16] or nickel sequestration [17], the reduction of halogenated methanes [18], trichloroethane [19], environmental DDT [20], and poly-chlorinated biphenyls [21]. Nanoscale zero valent colloidal iron has also been proposed for the removal of arsenic from drinking water [22]. The use of iron nanoparticles deposited at electrode surfaces has been reported very rarely and the lack of this kind of approach has been pointed out in a recent review [23]. In part, this lack of study in this important field is due to the high reactivity of iron deposits and the rapid formation of inert oxide coatings in aqueous envi-

* Corresponding author. Fax: +44 1225 386231.
E-mail address: f.marken@bath.ac.uk (F. Marken).

1388-2481/$ - see front matter © 2007 Elsevier B.V. All rights reserved.
doi:10.1016/j.elecom.2007.01.018

ronments. We have shown previously that hydrous iron oxide is bound very effectively onto and reduced at boron-doped diamond surfaces [24]. However, the conversion of the oxide deposit to iron metal in aqueous media has not been previously observed. In this study it is demonstrated that the presence of fluoride in aqueous media allows both iron metal formation and iron stripping processes at boron-doped diamond electrodes. Conventional anodic stripping voltammetry with trace amounts of aqueous iron is possible and iron deposits at boron-doped diamond electrodes are shown to be durable and catalytically active in electro-dehalognation processes.

Fluoride anion binding plays an important role in processes at the iron oxide–water interface, for example, for goethite [25] and for hematite [26]. The exchange of fluoride for hydroxide at the surface affects the ability of the oxide surface to passivate. It is shown here that in the presence of fluoride the surface of iron and iron oxide deposits remains electrochemically reactive. Water-soluble complexes of iron and fluoride are readily formed for both Fe^{2+} [27] and for Fe^{3+} [28]. The exchange of water against fluoride ligands occurs stepwise (leading to $FeF^{(n-1)+}$, $FeF_2^{(n-2)+}$, $FeF_3^{(n-3)+}$, etc.) [29] and may be incomplete in particular in acidic aqueous solution. Under conditions employed in this study (aqueous 1 M NH_4F electrolyte) it is assumed that the $FeF_6^{3-/4-}$ species predominates although $FeF_5(OH_2)^{2-/3-}$ and similar aquo species may still be present and important.

This study addresses mechanistic aspects of the formation of iron nanoparticle decorated boron-doped diamond electrodes and their reactivity. In order to study the deposition and stripping or iron, sonoelectrochemical methods [30,31] with considerably enhanced mass transport are employed. The deposition procedure and the demonstration of catalytic reactivity of iron deposits in this report will be of considerable future use, for example, in electroanalysis or in iron catalysed sonoelectrochemical dehalogenation and decontamination processes.

2. Experimental

2.1. Chemical reagents

NH_4F, $Fe(NO_3)_3$, EDTA, sodium dithionite, sodium trichloroacetate, sodium dichloroacteate, and sodium monochloroacetate were obtained commercially (Aldrich) in the purest available grade. Demineralised and filtered water of resistivity not less than 18 MOhm cm was taken from an Elga water purification system. Argon (Pure shield, BOC) was used for de-aeration of electrolyte solutions.

2.2. Instrumentation

A conventional three-electrode micro-Autolab III potentiostat system (Eco Chemie, NL) was employed to control the potential at the working electrode. The counter electrode was platinum gauze (1 cm^2) and the reference electrode was a KCl saturated Calomel electrode (SCE, Ref 401, Radiometer). The working electrode was a 3 mm diameter boron-doped diamond electrode (Diafilm, Windsor Scientific, UK) and in some cases a 3 mm diameter glassy carbon electrode (BAS, USA). Scanning electron microscopy images were obtained on a JEOL JSM6310 system. Prior to imaging, samples were gold sputter coated to improve the image quality.

Sonoelectrochemical measurements were conducted in a 100 cm^3 three-necked cell with the working electrode fixed and opposite to the ultrasonic glass horn probe which is immersed from the top of the cell [32]. An ultrasonic processor (Hielscher UP 200 G, 24 Hz, 200 W, maximum ultrasound intensity 8 W cm^{-2}) equipped with a 13 mm diameter glass horn was employed. The electrode to horn distance was kept constant at 5 mm and the maximum ultrasound intensity, 8 W cm^{-2}, was applied in all experiments. Ultrasound was only applied for short periods of time to prevent the temperature of the solution in the electrochemical cell from rising significantly above room temperature ($T = 22 \pm 2$ °C). High purity argon (BOC) was employed to thoroughly de-aerate all solutions prior to experiments.

2.3. Sonoelectrochemical mass transport calibration

In order to quantify mass transport effects introduced by ultrasonic agitation, a calibration procedure has been employed. The $Fe(CN)_6^{3-/4-}$ redox system provides a reversible one-electron reference system in aqueous 1 M NH_4F. Fig. 1a shows a typical cyclic voltammogram obtained for the reduction and re-oxidation of 5 mM $Fe(CN)_6^{3-}$ in 1 M NH_4F at a 3 mm diameter boron-doped diamond electrode. The reversible potential is 0.25 V vs. SCE and the peak-to-peak separation 76 mV at a scan rate of 0.2 V s^{-1} consistent with close to reversible electron transfer. A plot of the cathodic peak current versus the square root of scan rate is linear and allows the diffusion coefficient for the $Fe(CN)_6^{3-}$ anion in this medium, $D_{Fe(CN)_6^{3-}} = 0.48(\pm 0.02) \times 10^{-9}$ m^2 s^{-1}, to be obtained [33]. Next, chronoamperograms were recorded in order to determine the mass transport controlled limiting current under ultrasound conditions and as a function of the electrode to horn distance (see Fig. 1b). The mass transport coefficient, k_m, based on Eq. (1) was determined and is plotted versus the electrode to horn distance in Fig. 1c,

$$i_{lim} = nFk_m c \quad (1)$$

In this equation i_{lim} is the average mass transport controlled limiting current density, n is the number of electrons transferred per molecule diffusing to the electrode surface, F is the Faraday constant, and c is the bulk concentration of $Fe(CN)_6^{3-}$ in the solution.

From the calibration data it can be seen that good mass transport enhancement effects are observed for an electrode to horn distance of 5 mm with an average $k_m = 7.5 \times 10^{-5}$ m s^{-1}. Therefore, all sonoelectrochemical exper-

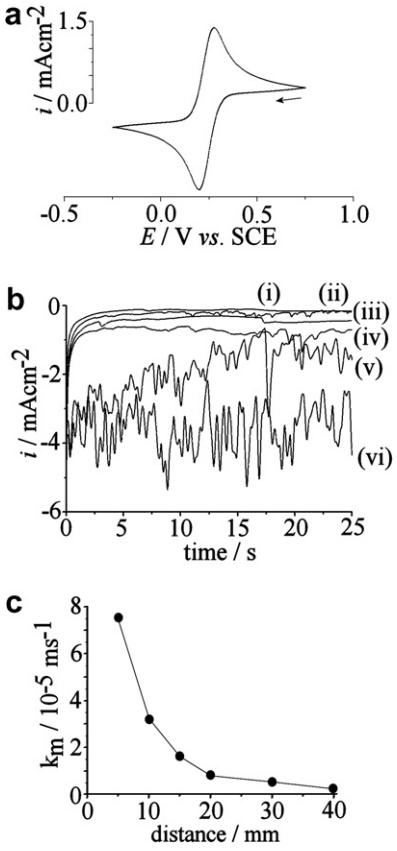

Fig. 1. (a) Cyclic voltammogram (scan rate 0.2 V s^{-1}) for the reduction and re-oxidation of 5 mM $Fe(CN)_6^{3-}$ in aqueous 1 M NH_4F at a 3 mm diameter boron-doped diamond electrode. (b) Chronoamperograms (applied potential 0.1 V vs. SCE, 8 W cm^{-2} ultrasound) for the reduction of 5 mM $Fe(CN)_6^{3-}$ in aqueous 1 M NH_4F with an electrode to horn gap of (i) 40, (ii) 30, (iii) 20, (iv) 15, (v) 10, and (vi) 5 mm. (c) Plot of the average mass transport coefficient obtained from the limiting current (8 W cm^{-2} ultrasound) versus the electrode to horn tip distance.

iments in this study were conducted with a fixed 5 mm electrode to horn distance. With the diffusion coefficient $D_{Fe(CN)_6^{3-}} = 0.48 \times 10^{-9}$ m^2 s^{-1} known, it is possible to obtain an estimate for the diffusion layer thickness under these conditions, $\delta = \frac{D_{Fe(CN)_6^{3-}}}{k_m} = 6.4$ μm. This value is in good agreement with literature reports [34] and consistent with strongly enhanced mass transport to the electrode surface.

2.4. Cleaning procedure for the removal of iron from the boron-doped diamond electrode surface

After repeated use of boron-doped diamond electrodes in iron stripping voltammetry experiments, it was observed that iron remained strongly immobilized at the electrode surface (presumably in the form of residual oxides formed during stripping). Nitric acid (prolonged exposure to hot or cold 0.5 M HNO_3) did not remove these deposits and residual stripping peaks were observed even in the absence of FeF_6^{3-} in solution. However, immersion of the electrode into an aqueous solution of 50 mM sodium dithionite and 0.5 M EDTA overnight completely removed iron and resulted reliably in a clean background voltammogram in aqueous 1 M NH_4F.

3. Results and discussion

3.1. The electro-deposition and stripping of iron: reactivity in aqueous fluoride media

After scanning the working electrode potential to −1.5 V vs. SCE a clean boron-doped diamond electrode immersed in aqueous 1 M NH_4F solution containing 10 μM FeF_6^{3-} shows a well defined stripping response at −0.58 V vs. SCE (see Fig. 2, curve ii). In the absence of FeF_6^{3-} no peak is observed (see Fig. 2, curve i) and by varying the FeF_6^{3-} concentration (see below) the peak feature can be clearly identified as iron stripping. The stripping process is tentatively assigned to a three-electron process (vide infra).

$$Fe(metal) + 6F^-(aq) \rightarrow FeF_6^{3-}(aq) + 3e^- \quad (2)$$

The process is highly sensitive to low concentrations of iron (down to sub-μM concentrations) and requires both (i) the boron-doped diamond electrode and (ii) the presence of 1 M NH_4F. Similar experiments with a glassy carbon working electrode replacing boron-doped diamond or with lower concentrations of NH_4F were not successful. When conducted in the presence of ultrasound, the considerable mass transport enhancement of the cathodic process can be seen (see Fig. 2, curve iii).

The cathodic current in the presence of ultrasound increases rapidly and at potentials of ca. −1 V vs. SCE due to the formation of an active catalyst layer (presumably iron metal) at the electrode surface. The increased noise level (due to turbulent interfacial convection) is indicative of mass transport control. The limiting current observed after reversal of the scan direction can be analysed based on Eq. (1) to give the approximate number of electrons transferred in this process. From the average limiting current density of 10 μA cm^{-2} and $k_m = 7.5 \times 10^{-5}$ m s^{-1} (see Section 2) the number of electrons transferred, $n = 1$ is obtained. The process is consistent with the one-electron reduction of FeF_6^{3-}.

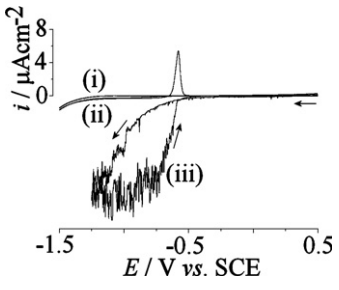

Fig. 2. Cyclic voltammograms (scan rate 0.02 V s^{-1}) obtained at a 3 mm diameter boron-doped diamond electrode in aqueous 1 M NH_4F: (i) background, (ii) in the presence of 10 μM FeF_6^{3-}, (iii) in the presence of 10 μM FeF_6^{3-} and 8 W cm^{-2} ultrasound (5 mm horn to electrode distance).

$$FeF_6^{3-}(aq) + e^- \rightleftarrows FeF_6^{4-}(aq) \quad (3)$$

This process is not observed at the bare boron-doped diamond electrode and it is likely that this electron transfer process is catalysed by the presence of iron metal or iron oxide at the electrode surface. The absence of a direct reduction response for FeF_6^{3-} at bare boron-doped diamond may be associated with very slow electron transfer kinetics associated for example with the spin states in $FeF_6^{3-/4-}$. From data in Fig. 2 the reversible potential for the $FeF_6^{3-/4-}$ redox system can be estimated as ca. −0.6 V vs. SCE. Interestingly, the peak feature for the iron stripping process is suppressed in the presence of ultrasound (see Fig. 2, curve iii) presumably due to (i) the more positive switching potential of −1.2 V vs. SCE and (ii) the fast mass transport leading to rapid comproportionation:

$$Fe(metal) + 2FeF_6^{3-}(aq) \rightleftarrows 3FeF_6^{4-}(aq) \quad (4)$$

Due to the intermediate Fe(II) redox state, iron stripping processes are mechanistically more complex when compared to more simple electrochemical stripping processes. The direct stripping of the iron deposit to give the reduced form FeF_6^{4-} at a more negative potential appears kinetically unfavorable (vide infra).

3.2. The electro-deposition and stripping of iron: deposition potential and time effects

Next, the effect of the deposition potential on the stripping peak feature is investigated. Linear scan voltammetry experiments are performed with a 30 s deposition time followed by a scan to positive potentials. Fig. 3a shows that the iron stripping peak is characteristically dependent on the deposition potential. The peak is first observed at a deposition potential of −1 V vs. SCE (with 30 s deposition) and a systematic increase is seen at more negative deposition potentials. However, a complication arises at potentials negative of −1.6 V vs. SCE where the stripping peak broadens. The reason for the broadening is currently unknown but it can be avoided in the presence of ultrasound.

In the presence of continuous ultrasound (24 kHz, 8 W cm^{-2}, 5 mm electrode to horn distance) a much improved stripping peak is detected (see Fig. 3b). In contrast to data shown in Fig. 2, here the deposition process is more dominant and loss of the stripping signal due to comproportionation appears to be insignificant. Due (at least in part) to fast mass transport in the presence of ultrasound the stripping peaks are typically 50-fold increased and highly symmetric even with more negative applied deposition potentials. A mass transport limit for the iron deposition process is not reached even at potential as low as −2 V vs. SCE.

The plot in Fig. 3c demonstrates the strong effect of ultrasonic agitation on the deposition process and the continuing increase of the stripping response at more negative deposition potentials. However, the charge under the peak observed with a deposition potential of −2 V vs. SCE

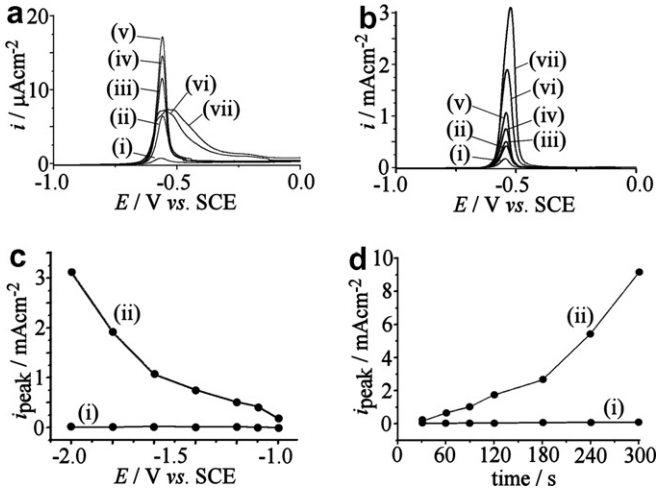

Fig. 3. (a) Linear scan voltammograms (scan rate 0.1 V s^{-1}, deposition potential: (i) −1.0, (ii) −1.1, (iii) −1.2, (iv) −1.4, (v) −1.6, (vi) −1.8, and (vii) −2.0 V vs. SCE, deposition time 30 s) for the stripping of iron deposited in 10 μM FeF_6^{3-} in 1 M NH_4F at a 3 mm diameter boron-doped diamond electrode. (b) Conditions as in (a) but with continuous 8 W cm^{-2} ultrasound (5 mm horn to electrode distance) applied. (c) Plot of the peak current for the iron stripping response versus deposition potential for (i) silent conditions and (ii) ultrasound conditions. (d) Plot of the peak current for iron stripping versus deposition time for (i) silent conditions and (ii) ultrasound conditions.

(Fig. 3b) is very close to that predicted (based on Eq. (1)) for diffusion controlled deposition and a further increase is unlikely.

Next, the effect of the deposition time has been investigated in the absence and in the presence of ultrasound. Fig. 3d clearly demonstrates the effect of continuing deposition, in particular with fast mass transport. The iron stripping peak is significantly further increased.

In order to investigate the deposit formed under optimized conditions, SEM images of the boron-doped diamond surface with iron deposits were obtained. Fig. 4 shows images in which a scratch line allows the boron-doped diamond base to be distinguished from the deposit. A nanoparticulate material with approximately 20–30 nm particle diameter is observed after 600 s sonoelectrochemical deposition at −1.5 V vs. SCE in a solutions containing 10 μM FeF_6^{3-} and 1 M NH_4F.

3.3. The electro-deposition and stripping of iron: concentration effects

Next, the effect of the iron concentration on the electrodeposition and stripping processes is investigated. Rather than further reducing iron levels, here the effects of a higher iron concentration are explored. Fig. 5a shows linear scan voltammograms obtained after 30 s deposition and for various levels of FeF_6^{3-} concentrations. Overall a more complex behaviour is observed although the stripping peak clearly increases with FeF_6^{3-} concentration.

Increasing the FeF_6^{3-} concentration initially results in a non-linear increase in the stripping peak current. However, at a concentration of 0.3 mM and higher the shape of the

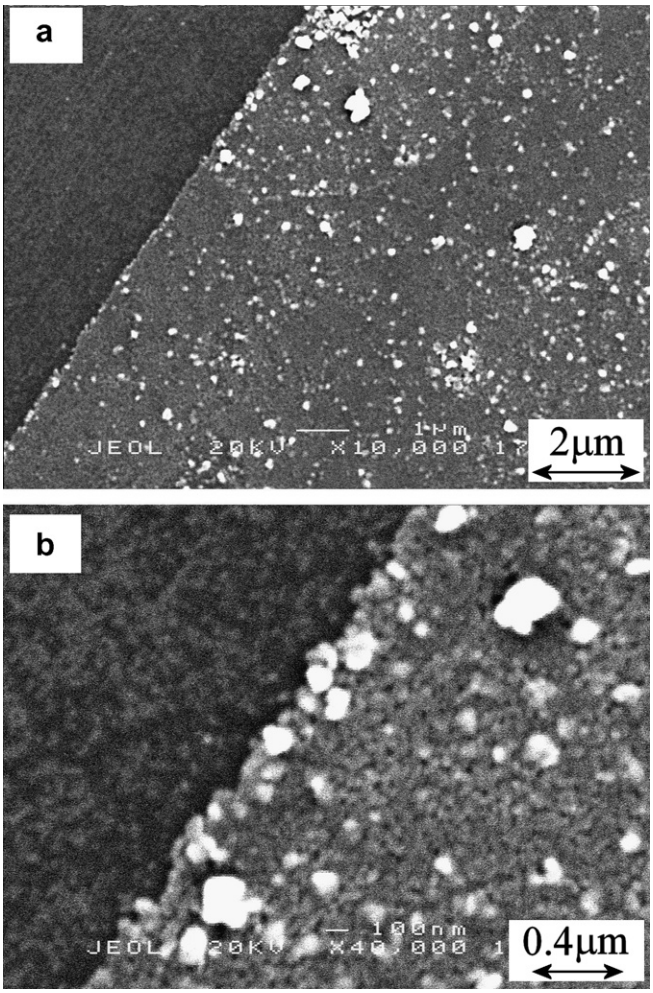

Fig. 4. (a) Scanning electron micrographs for an iron deposit on boron-doped diamond (generated by deposition at −1.5 V vs. SCE for 600 s with 8 W cm^{-2} ultrasound immersed in 10 μM FeF_6^{3-} in 1 M NH_4F. (b) Higher magnification image showing individual nanoparticles. Samples were scratched and gold sputter coated prior to imaging to improve image quality.

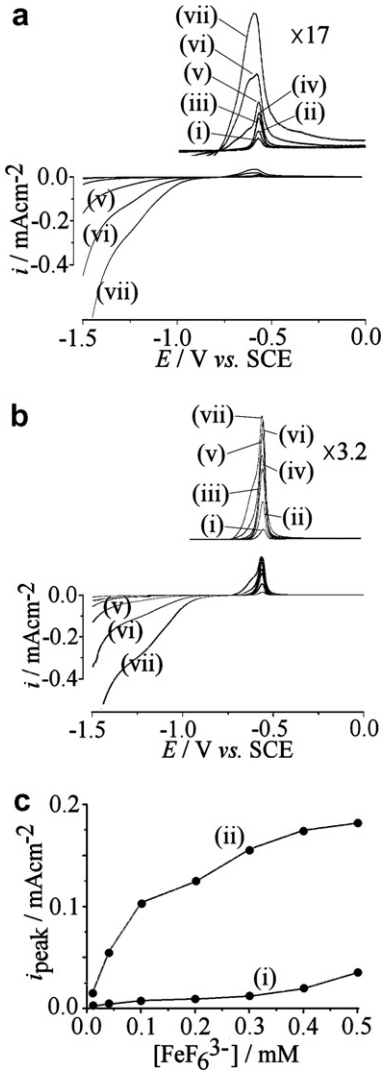

Fig. 5. (a) Linear scan voltammograms (scan rate 0.1 V s^{-1}, deposition potential −1.5 V vs. SCE, deposition time 30 s) for the stripping of iron deposited in (i) 10, (ii) 40, (iii) 100, (iv) 200, (v) 300, (vi) 400, and (vii) 500 μM FeF_6^{3-} in 1 M NH_4F at a 3 mm diameter boron-doped diamond electrode. (b) Conditions as in (a) but with continuous 8 W cm^{-2} ultrasound (5 mm electrode to horn distance) applied. (c) Plot of the peak current for iron stripping vs. FeF_6^{3-} concentration for (i) silent conditions and (ii) ultrasound conditions.

peak is changed and the stripping process appears to commence already at a more negative potential. Closer inspection of Fig. 5a shows that there is a distinct point at ca. −0.6 V vs. SCE where the current crosses from negative to positive. The presence of a higher concentration of FeF_6^{3-} appears to enhance the electro-dissolution kinetics for iron possibly due to interaction with the surface of the deposit. The overall mechanism for this process is currently not well understood and additional work for example with in situ quartz crystal microbalance mass sensors or spectro-electrochemical tools will be required to provide further insight into the kinetics of iron electro-dissolution processes under these conditions.

3.4. Catalytic reactivity of electro-deposited iron towards trichloroacetate

Iron is a highly catalytic metal with applications in a wide range of technical processes [35]. Often the state of the iron or iron oxide surface is important for controlling reactivity. Cathodic processes such as hydrogen evolution at iron alloys [36] and dehalogenation processes at iron metal particles [37] have been reported. Reduced forms of iron metal complexes such as hemin [38] or hemoglobin [39] also allow dehalogenation processes to proceed. Here, the reduction of the trichloroacetate anion may be regarded as a model system for the reductive electrodehalogenation process at active iron surfaces in the presence of fluoride.

In Fig. 6a cyclic voltammograms are shown recorded at a 3 mm diameter boron-doped diamond electrode immersed in a solution of 10 μM FeF_6^{3-} in 1 M NH_4F in the absence (i) and in the presence (ii) of 1 mM trichloroacetate. In the absence of FeF_6^{3-} no direct reduction

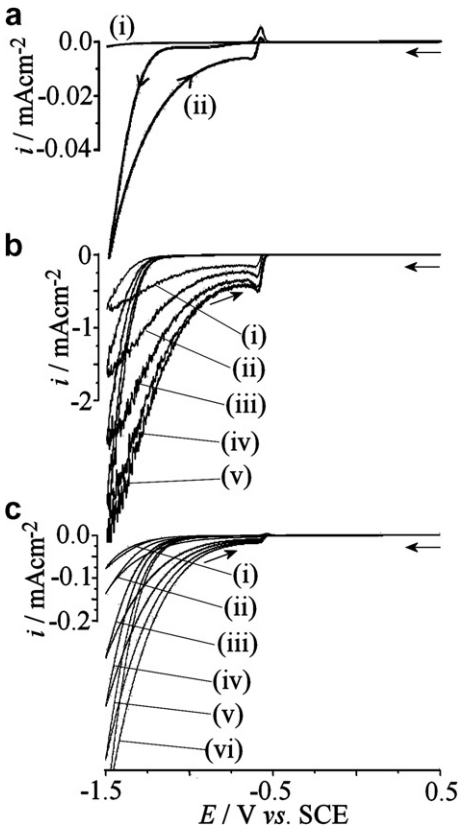

Fig. 6. (a) Cyclic voltammograms (scan rate 0.02 V s^{-1}) for the reduction and re-oxidation of 10 μM FeF_6^{3-} in 1 M NH_4F at a 3 mm diameter boron-doped diamond electrode (i) without and (ii) with 1 mM trichloroactate. (b) Conditions as in (a) and with (i) 1 mM, (ii) 2 mM, (iii) 3 mM, (iv) 4 mM, and (v) 5 mM trichloroacetate added and in the presence of continuous ultrasound (8 W cm^{-2}, 5 mm electrode to horn distance). (c) Cyclic voltammograms (scan rate 0.02 V s^{-1}) for the reduction and re-oxidation of immobilized iron at a 3 mm diameter boron-doped diamond electrode in 1 M NH_4F in the presence of (i) 0 mM, (ii) 1 mM, (iii) 3 mM, (iv) 5 mM, (v) 7 mM, and (vi) 9 mM trichloroactate.

response is observed even in the presence of higher concentration of trichloroacetate. The cathodic current in Fig. 6a(ii) is therefore catalytic.

The trichloroacetate reduction commences at a potential of ca. −0.8 V vs. SCE and then with increasing electrodeposition of iron the current increases at more negative potentials. Increasing the trichloroacetate concentration also increases the cathodic current. In the presence of trichloroacetate the iron stripping response is suppressed. In the presence of ultrasound (see Fig. 6b) cathodic currents are further increased. The cathodic peak feature at ca. −0.6 V vs. SCE is indicating a higher catalytic activity close to the potential where iron stripping would be observed in the absence of trichloroacetate. The noise level on the sonovoltammograms for trichloroactetate reduction is relatively low and therefore consistent with a process dominated by the kinetic rate of a chemical reaction step rather than by mass transport. The highest cathodic current observed for the reduction of 1 mM trichloroacetate, −0.75 mA cm^{-2}, is in first approximation consistent with a process with $n = 1$ (assuming mass transport control and using Eq. (1)). However, this appears unreasonable and further experiments with dichloroacetate and monochloroacetate (not shown) which also result in catalytic cathodic currents in the presence of iron suggest (consistent with literature reports [40,41]) that overall a stepwise multi-electron reduction and dechloronation ultimately down to acetate (Eq. (5)) is likely to occur,

$$Cl_3CCO_2^-(aq) + 3H_2O + 6e^- \rightleftarrows H_3CCO_2^-(aq) + 3Cl^-(aq) + 3OH^- \quad (5)$$

These processes have been observed in the presence of added FeF_6^{3-} and they rely on iron deposition prior to electrocatalysis. However, perhaps surprisingly, the catalytically active deposit of iron is often not fully removed during the anodic stripping process and stable oxide films may form. The formation of oxide intermediates appears to be facile and the removal of all iron from the electrode surface after use required a special cleaning procedure (see Experimental) based on dithionite and EDTA. This observation is consistent with a strongly adhering pre-catalyst film (which is activated during reduction) at the boron-doped diamond electrode surface. Indeed, experiments with an iron modified boron-doped diamond electrode in trichloroacetate containing solution (see Fig. 6c) demonstrate that currents similar to those obtained in the presence of FeF_6^{3-} are obtained even in the absence of intentionally added FeF_6^{3-}. Therefore, this kind of iron or iron oxide modified boron-doped diamond electrode maintains its catalytic activity and in future it will be possible to transfer and apply this catalyst-modified electrode into a wider range of aqueous electrolyte solutions, perhaps even without fluoride, and for a wider range of catalytic dehalogenation processes.

4. Conclusions

It has been demonstrated that iron is reversibly electrodeposited and stripped at boron-doped diamond electrodes immersed into aqueous 1 M NH_4F solution. A very sensitive stripping response is obtained even at very low concentrations of FeF_6^{3-} and the effects of concentration, deposition time, and deposition potential have been reported. The iron deposit has been demonstrated to provide electro-catalytic activity towards cathodic dehalogenation processes. Processes such as the reduction of trichloroacetate are facile in the presence of iron at the boron-doped diamond electrode surface. Further work on this system for potential analytical applications and on the benefits of iron for clean sonoelectrocatalytic dehalogenation or decontamination processes is in progress.

Acknowledgements

This work was supported by the EU COST Programme (Action D32, working groups "Microwave and Ultrasound Activation in Chemical Analysis" and "Electrochemistry

with Ultrasound''). V.S. and J.G.-G. thank the Generalidad Valenciana for the financial support by the Project GV05/104.

References

[1] A. Fujishima, Y. Einaga, T.N. Rao, D.A. Tryk, Diamond Electrochemistry, Elsevier, Amsterdam, 2005.
[2] M. Hupert, A. Muck, R. Wang, J. Stotter, Z. Cvackova, S. Haymond, Y. Show, G.M. Swain, Diam. Relat. Mater. 12 (2003) 1940.
[3] R.G. Compton, J.S. Foord, F. Marken, Electroanal. 15 (2003) 1349.
[4] J.S. Gao, T. Arunagiri, J.J. Chen, P. Goodwill, O. Chyan, J. Perez, D. Golden, Chem. Mater. 12 (2000) 3495.
[5] A. De Battisti, S. Ferro, M. Dal Colle, J. Phys. Chem. B 105 (2001) 1679.
[6] F. Montilla, E. Morallon, I. Duo, C. Comninellis, J.L. Vazquez, Electrochim. Acta 48 (2003) 3891.
[7] S. Szunerits, C. Jarna, Y. Coffinier, B. Marcus, D. Delabouglise, R. Boukherroub, Electrochem. Commun. 8 (2006) 1185.
[8] I. Yagi, T. Ishida, K. Uosaki, Electrochem. Commun. 6 (2004) 773.
[9] B. El Roustom, G. Foti, C. Comninellis, Electrochem. Commun. 7 (2005) 398.
[10] G. Sine, I. Duo, B. El Roustom, G. Foti, C. Comninellis, J. Appl. Electrochem. 36 (2006) 847.
[11] F. Marken, A.S. Bhambra, D.H. Kim, R.J. Mortimer, S.J. Stott, Electrochem. Commun. 6 (2004) 1153.
[12] S. Ferro, A. De Battisti, J. Phys. Chem. B 106 (2002) 2249.
[13] K.J. McKenzie, F. Marken, Electrochem. Solid St. 5 (2002) E47.
[14] N. Spataru, C. Terashima, K. Tokuhiro, I. Sutanto, D.A. Tryk, S.M. Park, A. Fujishima, J. Electrochem. Soc. 150 (2003) E337.
[15] C. Terashima, T.N. Rao, B.V. Sarada, N. Spataru, A. Fujishima, J. Electroanal. Chem. 544 (2003) 65.
[16] Y.P. Sun, X.Q. Li, J.S. Cao, W.X. Zhang, H.P. Wang, Adv. Colloid Interf. 120 (2006) 47.
[17] X.Q. Li, W.X. Zhang, Langmuir 22 (2006) 4638.
[18] H. Song, E.R. Carraway, Environ. Eng. Sci. 23 (2006) 272.
[19] W.S. Orth, R.W. Gillham, Environ. Sci. Technol. 30 (1996) 66.
[20] T. Eggen, A. Majcherczyk, Chemosphere 62 (2006) 1116.
[21] C.M. Li, T.C. Chen, K.H. Chiu, H.K. Yak, Surf. Sci. 600 (2006) 1382.
[22] S.R. Kanel, J.M. Greneche, H. Choi, Environ. Sci. Technol. 40 (2006) 2045.
[23] C.W. Welch, R.G. Compton, Anal. Bioanal. Chem. 384 (2006) 601.
[24] K.J. McKenzie, D. Asogan, F. Marken, Electrochem. Commun. 4 (2002) 820.
[25] T. Hiemstra, W.H. Van Riemsdijk, J. Colloid. Interf. Sci. 225 (2000) 94.
[26] W. Stumm, J.J. Morgan, Aquatic Chemistry, Wiley, New York, 1996.
[27] G.A. Nazmutdinova, V.G. Shtyrlin, A.V. Zakharov, Y.I. Sal'nikov, Koordinats. Khim. 19 (1993) 701.
[28] H.W. Dodgen, G.K. Rollefson, J. Am. Chem. Soc. 71 (1949) 2600.
[29] A.J. Edwards, J. Chem. Soc. Dalton Trans. (1972) 816.
[30] R.G. Compton, J.C. Eklund, F. Marken, Electroanal. 9 (1997) 509.
[31] K.B. Holt, J. Del Campo, J.S. Foord, R.G. Compton, F. Marken, J. Electroanal. Chem. 513 (2001) 94.
[32] K.B. Holt, G. Sabin, R.G. Compton, J.S. Foord, F. Marken, Electroanalysis 14 (2002) 797.
[33] F. Scholz, Electroanalytical Methods, Springer, 2002.
[34] F. Marken, R.P. Akkermans, R.G. Compton, J. Electroanal. Chem. 415 (1996) 55.
[35] W.X. Zhang, J. Nanoparticle Res. 5 (2003) 323.
[36] F. Rosalbino, D. Maccio, E. Angelini, A. Saccone, S. Delfino, J. Alloys Compd. 403 (2005) 275.
[37] T.L. Johnson, M.M. Scherer, P.G. Tratnyek, Environ. Sci. Technol. 30 (1996) 2634.
[38] J.R. Stromberg, J.D. Wnuk, R.A.F. Pinlac, G.J. Meyer, Nanoletters 6 (2006) 1284.
[39] Y.P. Li, H.B. Cao, Y. Zhang, Chemosphere 63 (2006) 359.
[40] J. Yang, N. Hu, Bioelectrochem. Bioenerg. 48 (1999) 117.
[41] I.A. Avrutskaya, T.A. Arkhipova, G.V. Itov, N.E. Krasnoshchekova, Elektrokhimiya 29 (1993) 926.